

PAPER

Design, fabrication and experimental verification of a drag sail based on thermal-driven controllable bi-stable shape memory polymer composite booms

To cite this article: Guangqing Ming *et al* 2024 *Smart Mater. Struct.* **33** 055040

View the [article online](#) for updates and enhancements.

You may also like

- [\(Poster Award - 3rd Place\) Synthesis of Spherical Mesoporous Carbon \(SMPC\) Support and Electrochemical Properties of Pt/SMPC Catalyst](#)
Sorataka Yoshikawa, Minyoung Kim, Hideo Inoue *et al.*
- [Ground and geostationary orbital qualification of a sunlight-stimulated substrate based on shape memory polymer composite](#)
Fengfeng Li, Liwu Liu, Xin Lan *et al.*
- [Elastocaloric effects of carbon fabric-reinforced shape memory polymer composites](#)
Seok Bin Hong, Yongsan An and Woong-Ryeol Yu

PRIME
PACIFIC RIM MEETING
ON ELECTROCHEMICAL
AND SOLID STATE SCIENCE




HONOLULU, HI
October 6-11, 2024

Joint International Meeting of
The Electrochemical Society of Japan (ECSJ)
The Korean Electrochemical Society (KECS)
The Electrochemical Society (ECS)

Early Registration Deadline:
September 3, 2024

**MAKE YOUR PLANS
NOW!**

Design, fabrication and experimental verification of a drag sail based on thermal-driven controllable bi-stable shape memory polymer composite booms

Guangqing Ming¹ , Siling Chen², Bingxun Li², Fengfeng Li^{2,*} , Liwu Liu² , Yanju Liu²  and Jinsong Leng^{1,*} 

¹ Center for Composite Materials and structures, Harbin Institute of Technology (HIT), PO BOX 3011, No. 2 Yikuang Street, Harbin 150080, People's Republic of China

² Department of Astronautical Science and Mechanics, Harbin Institute of Technology (HIT), PO Box 301, No. 92 West Dazhi Street, Harbin 150001, People's Republic of China

E-mail: lifengfeng@hit.edu.cn and lengjs@hit.edu.cn

Received 12 October 2023, revised 19 February 2024

Accepted for publication 11 April 2024

Published 22 April 2024



CrossMark

Abstract

Deployable drag sails are used for passively deorbiting defunct satellites and other spacecraft. Designing the deployable boom is the main challenge in this technology. We present a bi-stable shape memory polymer composite (Bi-SMPC) boom with high stiffness, a high unfolding/folding ratio, and consistent roll-out deployment. It was designed and fabricated by a strategy of controlling the gradual release of elastic energy stored in a bi-stable composite structure through thermal-driven SMP matrix. Two heating layer strategies were investigated experimentally to determine the optimal driving layer and driving parameters. Based on these parameters, verification tests of a four-stage deployment Bi-SMPC boom were conducted. Meanwhile, a proof-of-concept prototype of a four-stage deployment drag sail based on the Bi-SMPC booms was designed and fabricated. Tests were conducted to verify the effectiveness of the drag sail deployed by the booms. It was found that SMPs can effectively control the deployment of bistable composite structures. The nickel-chromium alloy heating layer offers a more uniform driving temperature field compared to carbon fiber. The drag sail can be deployed successfully under the driving of four Bi-SMPC booms.

Supplementary material for this article is available [online](#)

Keywords: deployable drag sail, deployment control, shape memory polymer, bi-stable structures, smart materials and structures

1. Introduction

The space environment is becoming more and more crowded. Especially in the low-earth orbit region, full of abandoned

satellites, rockets, and space debris formed by their collisions and explosions. As of 11 August 2022, data from ESA's Space Debris Office [1] shows that since 1957, 6250 rocket launches and 13 630 satellites have been sent into space. Only 6200 are still active. 31 400 pieces of space debris are tracked, and models predict over 36 500 larger than 10 cm, 1 million between 1–10 cm, and 130 million between 1 mm–1 cm. Over 630 events

* Authors to whom any correspondence should be addressed.

generate debris, mainly due to break-ups, explosions, collisions, etc. These accidents are currently the primary source of space debris [2, 3]. People deal with space debris by avoiding, protecting, mitigating, and removing it [4]. Preventive measures are insufficient, as debris growth outpaces removal [5]. Mitigation and removal are crucial, especially for decommissioned spacecraft. Accelerated re-entry is a fundamental way to reduce debris [6, 7].

The de-orbit methods of spacecraft include active de-orbit and passive de-orbit [4]. The former uses a power device carried by spacecraft to change orbit altitude and re-entry into the atmosphere. In contrast, the latter uses deployable film sails, electric power tethers, or inflatable balls to increase flight resistance to achieve deceleration and re-enter the atmosphere. Among them, the deployable film sail has excellent development potential due to its simple structure, light weight, and low cost. Some prototypes of deployable film sail have been demonstrated, such as the NanoSail-D [8] carried by NASA's 3U CubeSat, the Aerodynamic End-of-Life De-orbiting System [9] developed by the University of Glasgow, and the University of Toronto's CanX-7 Satellite Mission for a 3U drag sail [10].

The deployable boom is the core driving and the supporting component of this kind of deployable film sail [11–14]. Most deployable booms are made of thin-walled elastic materials such as carbon fiber composites and spring tape [15–17]. Their storage and release of the elastic energy are used to realize the folding and deploying. However, the deploying path of these booms driven only by releasing elastic energy is often disordered and difficult to predict, which is easy to cause the sail at risk of getting stuck or tearing the film. While for large-size deployable structures, a more complex control mechanism is usually needed to control the release of elastic energy for controlling the deployment speed and sequence.

Shape memory polymers (SMPs) are a type of smart materials that can respond to external stimuli such as light, heat, and magnetism [18, 19]. They have excellent mechanical properties in their glassy state and outstanding large deformability in their rubbery state. When heated above the glass-transition temperature (T_g), they can be shaped into a temporary shape by external forces and then memorize it as the temperature drops below T_g . When the temperature rises again above T_g , they can return to their original shape. The shape memory characteristics of SMPs provide possibilities for the design of large deformable and deployable structures. Thus, SMPs are widely used in various fields, including aerospace, smart actuators, and biomedicine [20–24]. The deploying process of deployable structures actuated by SMP is slower, low impact, and more controlled than traditional elastic or bi-stable structures, as compared in supplementary video S1. Because of these advantages of SMPs, some research has occurred on elastic or bi-stable deployable structures combined with SMPs [25–28].

In this study, we proposed a deployable bi-stable SMP composite (Bi-SMPC) boom with multifunction layers: a fiber reinforced layer, an elastic trigger layer, a deployment control

matrix, and a resistive heating layer. Anti-symmetric lay-up of fiber reinforced layer provides bi-stable deployment properties in the composites, and spring tape compounded inside the material is used as the bi-stable transition trigger source. The thermally driven SMP matrix controls the deployment speed and process of the Bi-SMPC boom driven by the resistive heating layer. Such a design strategy can realize a staged, orderly, and controllable deployment of the boom. Then heating layer of the Bi-SMPC boom was investigated by comparing the effectiveness and uniformity of two heating strategies, carbon fiber and alloy wire, as the heating layer. Furthermore, the Cr₂₀Ni₈₀ alloy wire was chosen as the heating source to verify the feasibility of deploying a four-stage Bi-SMPC boom. Meanwhile, a four-stage deployment drag sail based on the Bi-SMPC booms and origami folded film and its locking-release device and control module were designed and verified successfully.

2. Design and fabrication

2.1. Design and fabrication of the Bi-SMPC boom

The C-, Ω -, pod-shaped cross-sections have simple geometry and high moment of inertia and are widely used in space deployable booms. In this work, considering that small satellites' energy and space are limited, a simple C-shaped cross-section was adopted to design the Bi-SMPC boom. It can ensure that the boom has a small area for driving, good foldability, and considerable deployment stiffness. Table 1 shows the cross-section parameters used to design, fabricate, and practically verify the Bi-SMPC booms. The thickness depends on the carbon fiber layup, excluding the thickness of the heating layers and a 0.15 mm thick spring tape in the middle part.

Figures 1(a) and (b) show the detailed design and fabrication process of the Bi-SMPC boom. As shown in figure 1(a), the total length of the boom is 460 mm. The middle part of 435 mm is divided into four independent heating areas for segmental control of deployment and reducing driving power in practical applications. The ends of 15 mm and 10 mm of the boom are reserved for connecting with the central base and the connecting plate, respectively.

The components of the Bi-SMPC boom can be divided into the composites part and the resistive heating part. The composite part consists of two layers of carbon fabric with anti-symmetric layup used as reinforcement and bi-stable function layer, the epoxy-based SMP as the matrix to control the deployment of the boom, and an elastic 65Mn spring tape used as the trigger of the bi-stable structure deployment and meanwhile improving the driving force of the boom. The resistive heating part is a layer of resistive wire encapsulated by polyimide (PI) film. Resistive wires are arranged in the heating areas in an S-shape with a spacing of about 5 mm for heating the material evenly.

A two-step method was used to fabricate the Bi-SMPC boom: First, using Vacuum assisted resin infusion (VARI) process to gain Bi-SMPC without heating layers; second, using

Table 1. Cross section parameters of the boom.

Inside radius r	Arc length l	Central angle θ	Thickness t
20 mm	30 mm	86°	~0.32 mm

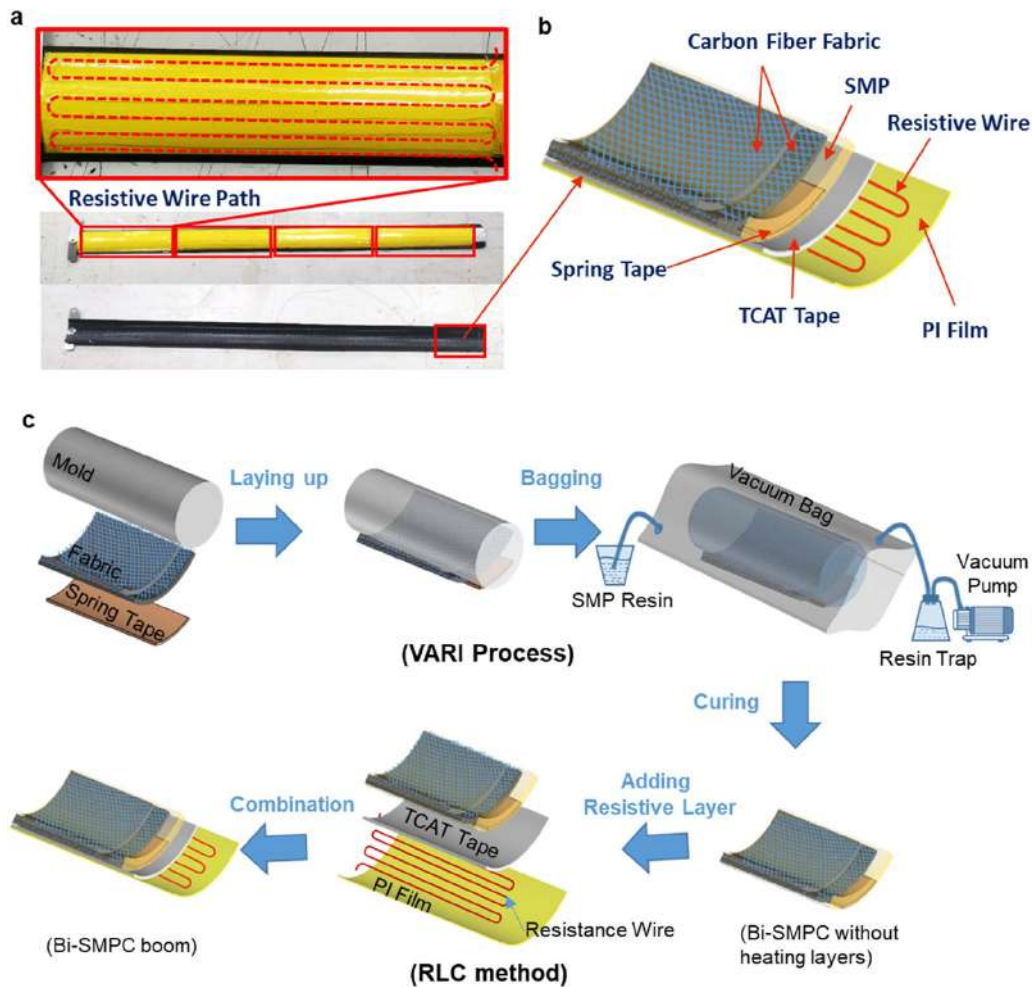


Figure 1. Design and fabrication of bi-stable shape memory polymer composite (Bi-SMPC) boom. (a) Front and back of the boom and the path of the resistive wire; (b) detail diagram of the layered structure of the Bi-SMPC boom; (c) fabrication process of the Bi-SMPC boom. (VARI: vacuum-assisted resin infusion; RLC: resistive layer combination; TCAT Tape: thermally conductive adhesive transfer tape).

resistive layer combination (RLC) method to assemble the heating layers, as shown in figure 1(c). Carbon fiber fabrics, spring tape, and the SMP resin were tightly combined through the VARI process to prevent delamination during the folding and deploying process of the boom with large strain variations. The RLC process provides a flexible heating circuit for driving the boom, during which 3M thermally conductive adhesive transfer tape (TCAT Tape) was used to bond the resistive wire and the PI insulation layer with the boom. The TCAT Tape filled with conductive ceramic fillers has excellent electrical insulation and thermal conductivity. Two resistive materials, Cr20Ni80 alloy wires and carbon fiber yarns, will be considered as the heating source, which will be investigated and compared in the supplementary material (sections S1 and S2).

2.2. Folding pattern design of the sail film

The drag sail film is made of a 600 mm × 600 mm square PI film with a thickness of 15 μm. It is easy to fold and rotate with the booms through practical crease design and local reinforcement of edges and can withstand specific preload after deployment. As shown in figure 2(a), the sail film is divided into four parts for easy folding and assembly, each of which is a right triangle but not an isosceles triangle due to the reserved space with a diameter of 30 mm at the center. The reserved space is used to install a central base, around which the films and booms will rotate and fold during the folding process. In the crease scheme diagram, Black lines represent the edges of the film or cuts; red lines represent mountain folds; and blue lines represent valley folds. Mountain and valley folds represent the direction of the crease, which are convex upwards and concave

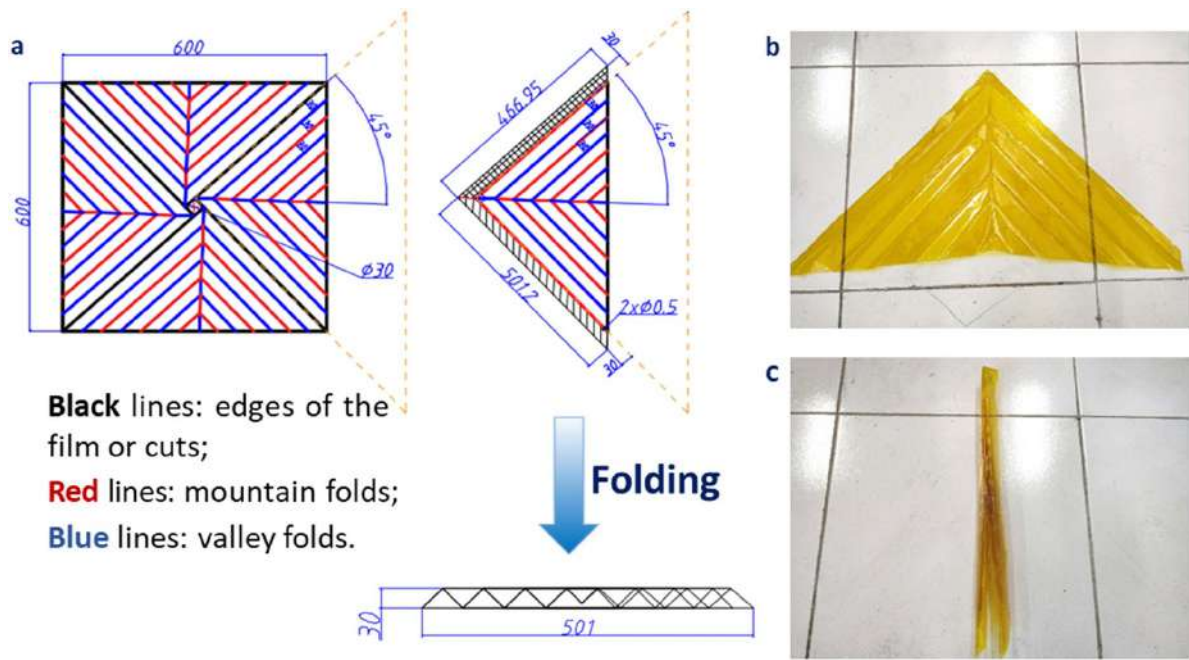


Figure 2. Folding scheme design of the sail film. (a) Schematic diagram of the folding scheme; (b) unfolded state of a triangle film; (c) folded state of a triangle film.

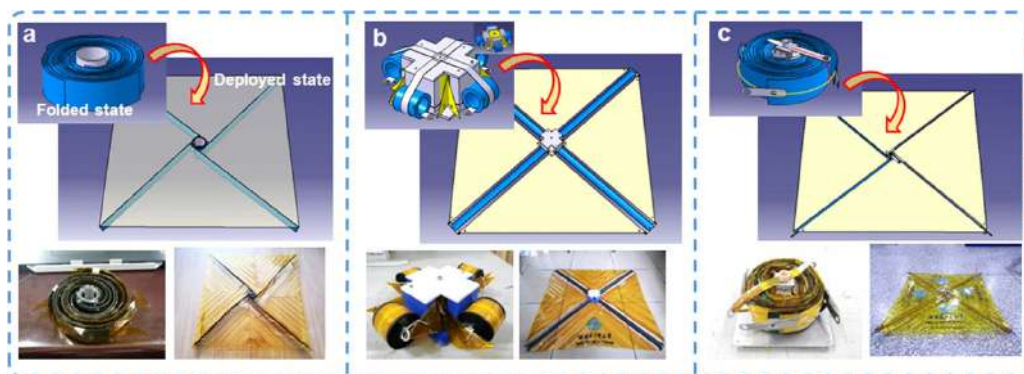


Figure 3. Design and comparison of three design schemes of the drag sail. (a)–(c) Models and prototypes for schemes (A)–(C), respectively.

downwards, respectively. Figures 2(b) and (c) are the unfolded state with creases and the fully folded state, respectively.

2.3. Deployable drag sail based on Bi-SMPC booms

2.3.1. Preliminary design. As shown in figures 3(a)–(c), there are three design schemes of the deployable drag sail at the preliminary design stage. All these schemes are square sails supported by four booms (blue in the figure). The main differences are the placement of the booms and the connection forms of the films (yellow in the figure) to the booms.

In scheme (A), four booms are placed perpendicular to the film's surface. Both right-angle edges of the film are fixed to the adjacent booms. The film is folded up simultaneously as the booms rotate and fold around the central base. In scheme (B), four booms are mounted parallel to the film's surface

and folded separately. The right-angle vertexes of the triangle films are fixed to the central box, and the acute-angle vertexes are attached to the tips of the booms. The four triangle sail films are folded and put into a central box. In scheme (C), four booms are placed perpendicular to the film's surface. One right-angle edge of each film is fixed on one boom, and the diagonal point is connected to another adjacent boom.

Three schemes were compared by main parameters, including the size of deployed and folded states, storage ratio, and weight, which are listed in table 2. It was found that (1) schemes (B) and (C) can easily fold the film and booms because the two parts were folded separately, but scheme (A) cannot; (2) scheme (C) is lighter than scheme (B), and the storage ratio is significantly improved by about 270%. This is due to the storage form of scheme (C) is more compact without carrying a film storage box which takes much space in

Table 2. Comparison of the three design schemes.

	Size of deployed state (mm)	Size of folded state (mm)	Storage ratio	Weight (g)	Connection forms between the films and booms
Scheme (A)	613 × 613 × 50	Φ 65 × 50	113	210	Two edges fixed
Scheme (B)	678 × 678 × 60	Φ150 × 60	26	230	Three points fixed
Scheme (C)	640 × 640 × 49	Φ 73 × 49	98	205	Single edge and one point fixed

scheme (B). Thus, scheme (C) was chosen for the follow-up study.

2.3.2. Detailed design and assembly. Based on scheme (C), a drag sail with a deployed size of 640 mm × 640 mm was designed and fabricated. It mainly composed of five parts: central base, deployable Bi-SMPC booms, PI film sail, locking structure, and control module. The volume of the folded sail is less than 0.5U (1U refers to a standard dimension of 10 cm × 10 cm × 10 cm for CubeSats). Overall design and details of the drag sail are shown in figure 4.

As details are shown in figure 4(c), Four booms are mounted to the central base. One right-angle edge of each triangular films is completely fixed to a boom, and the diagonal point of the fixed edge is connected to the tip of the adjacent boom through a spring connector. The function of the spring connector is to provide a specific preload for the deployed triangular film; meanwhile, it can be disconnected for easy operation when folding the sail.

Although the Bi-SMPC booms have good self-locking capabilities, the locking-release device has been designed to ensure the shock resistance reliability of the product in the launch stage. The locking-release device is composed of nylon locking rope, heat-cut alloy wire, spring sheet, and connecting plate, as shown in figure 4(a). The heat-cut alloy wire is prepared from Cr₂₀Ni₈₀ alloy. After the unlocking command is issued, the heat-cut alloy wire will be heated to over 200 °C, and the nylon locking rope passing through the connecting plate will melt and break. At the same time, the spring sheet will spring upwards to keep the heat-cut alloy wire away from the sail structure, and the unlocking process is completed and then waiting for the deployment command of the Bi-SMPC booms. The supplementary material (section S3) will experimentally investigate the driving parameters for the Bi-SMPC and the locking-release device, while the design of the control module can be found in the supplementary material (section S4).

3. Materials and methods

3.1. Materials and process for the composites

Two layers of carbon fiber fabric (T300, 1K, twill textile) with a [(±45)/(±45)] anti-symmetric stacking sequence, epoxy-based SMP resin developed by Leng's group [29] with

a T_g of 100 °C and 65Mn spring tape (0.12 mm thick and 16 mm wide) were used to fabricate the Bi-SMPC booms by vacuum assisted resin infusion (VARI) process. A stainless-steel tube with a diameter of 40 mm was used as a mold in the processing. An 80 °C/3 h-100 °C/3 h-150 °C/5 h step temperature procedure was used to cure the composites in an oven.

3.2. Materials for the heating layers

Cr₂₀Ni₈₀ alloy wire (0.25 mm in diameter, 22.21 Ω m⁻¹) and carbon fiber yarn (T300-12 K, 32.58 Ω m⁻¹) were used in the comparative investigation of two heating strategies. Cr₂₀Ni₈₀ alloy wire (0.15 mm in diameter, 61.68 Ω m⁻¹) was finally used as the resistive heating wire in the Bi-SMPC booms. The length of each part used in the heating circuit is about 600 mm, and the resistance is about 37 Ω. Varnished wire (QZY/XY-2, grade C) with a diameter of 0.2 mm was used in the heating circuit.

4. Simulation

4.1. Modeling of the drag sail

Simulation analysis was performed to verify that the deformation strain of the scheme was within an acceptable range and that would not cause damage to the composites during the deformation process. Explicit dynamics analysis was chosen to simulate the folding process due to the characteristics of large deformation and many contacts. The drag sail is simplified into three parts: a central base, Bi-SMPC booms, and 65Mn spring tapes. The central base is set as a rigid body and the other parts are set as deformable shells and they were tied together, as shown in figure 5. The two-layer [(±45)/(±45)] woven fabric SMPC booms are simplified into four-layer [±45/±45] unidirectional laminated composites, thus booms are set as layered structures with an [±45/±45] anti-symmetric stacking sequence.

The central base is set as the C3D8R elements and the booms and spring tapes are set as S4R elements. The mesh size is 2.5 mm, and the total number of elements is 20 352. The main parameters [30] used in the simulation are listed in table 3. The properties of SMPC are the values at its glass transition temperature of 100 °C.

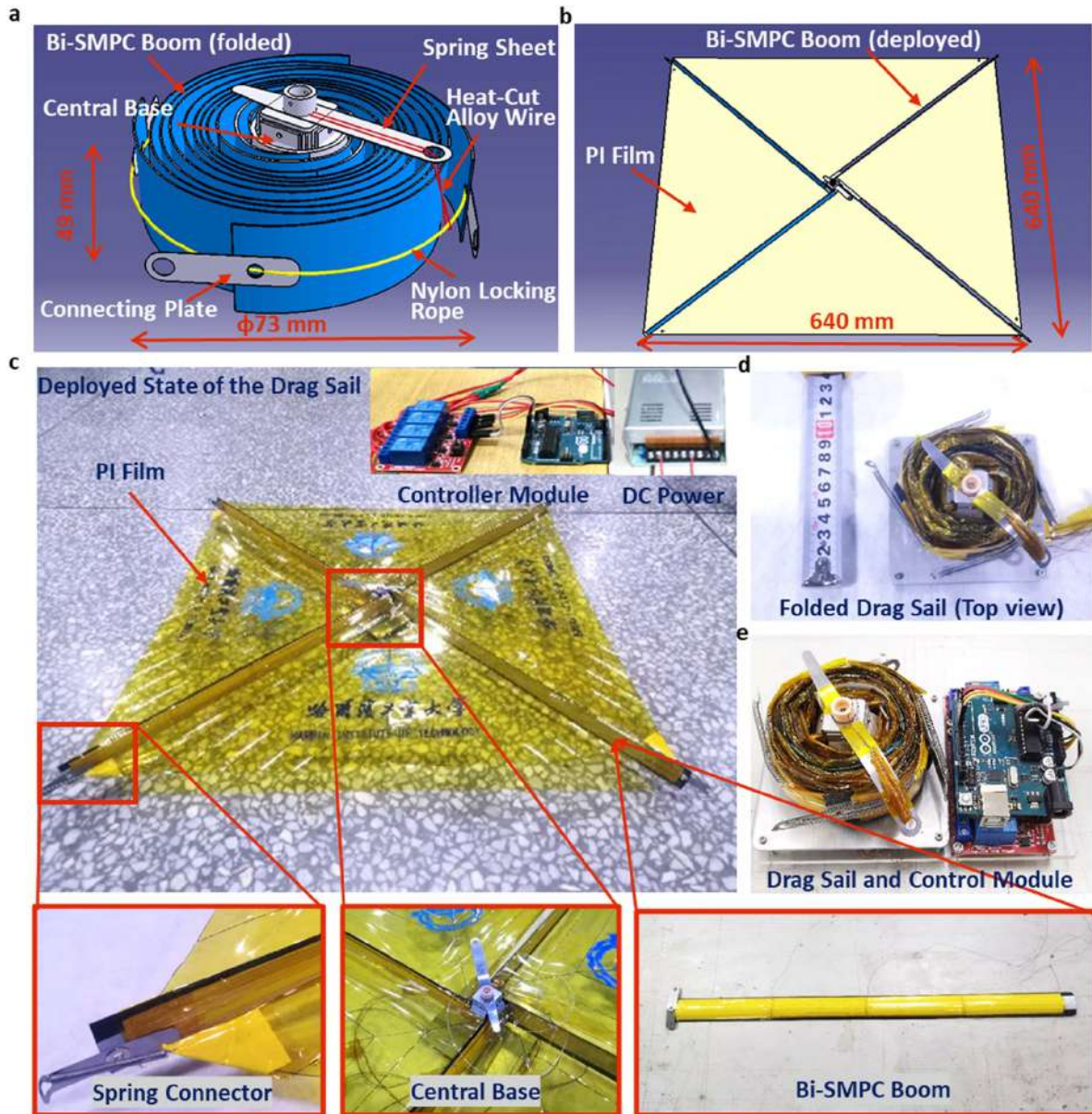


Figure 4. Design and assembly of the drag sail based on Bi-SMPC booms. (a) Geometric model of the folded drag sail; (b) geometric model of the deployed drag sail; (c) overall assembly and some details of the drag sail; (d) and (e) folded state of the drag sail and its control module.

4.2. Steps and boundary conditions

According to the practical folding process, a concentrated force of 30 N along the axial direction of the booms is applied to each tip of the booms during folding, as shown in figure 5(a). Meanwhile, rotation displacement is applied to the center bottom reference point of the central base to rotate the central base, so as to fold the booms. The contact property is set between the SMPC with a friction coefficient of 0.2. Table 4 lists the boundary condition of the central base at each step.

4.3. Simulation results

Figure 6 shows the logarithmic strain at each folding stage. It shows that the maximum strains of the structure at each

stage are 14.00%, 21%, 20.17%, and 19.88%, respectively. They all occur at the initial bending position marked in figure 6(b) and are within the deformability of the SMP resin (greater than 30% at T_g [31]). Thus, the folding can be realized, but special attention must be paid to the starting position due to the sharp cross-section shape change in the booms.

5. Experimental tests and discussion

5.1. Folding and deploying tests of the Bi-SMPC booms

In order to verify the design strategy of stimulating SMP to release bi-stable elastic energy of the boom for controlling the deployment and to obtain the effect of the heating layers on the

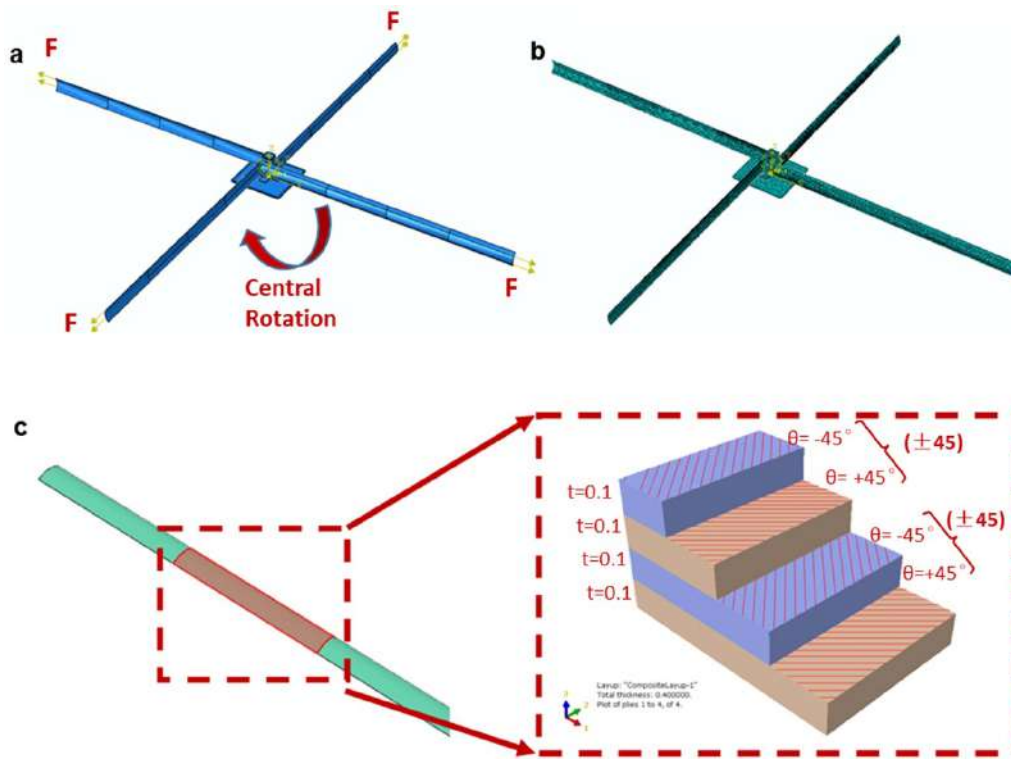


Figure 5. Modeling of the drag sail. (a) Simplified geometric model of the drag sail; (b) meshing of the drag sail; (c) diagram of the laminated structure in the Bi-SMPC.

Table 3. Material properties used in the simulation.

Material	Density (ton mm^{-3})	Modulus (MPa)					Poisson ratio	Thickness (mm)
Spring tape	7.8×10^9	209 000					0.27	0.12
SMPC (100 °C) [30]	1.5×10^9	E_1	E_2	G_{12}	G_{13}	G_{23}	μ_{12}	0.4
		5291	161	43	43	49	0.4	

Table 4. Boundary condition of the central base at each step.

Step	Initial angle (rad)	Angle after rotation (rad)
Step-1	0	4.8
Step-2	4.8	10.5
Step-3	10.5	16.1
Step-4	16.1	21.3

folding and deploying process of the Bi-SMPC boom, the folding and deploying tests of Bi-SMPC booms without and with a heating layer were conducted. The boom without a heating layer was heated in an oven.

(1) Folding test of the Bi-SMPC boom:

Both the naked Bi-SMPC boom and the boom with heating layer were placed in a 100 °C oven for 5 min, and then they were taken out and quickly folded into a five-tiered cylinder (inner diameter 20 mm, outer diameter 30.74 mm). After the

temperature cooled down to room temperature, they were kept in a folded state. Both booms had a 10%–15% elastic spring back after releasing the constraint which was used to hold the cylindrical boom. As shown in figure 7(a), the final folded cylindrical booms had an inner diameter of about 22 mm and an outer diameter of about 34.5 mm.

(2) Deploying test of the Bi-SMPC boom without heating layer:

As shown in figure 7(b), the Bi-SMPC boom without heating layer was placed in an oven to deploy. It can be found that the boom rolled out like a roller with only a tiny radial expansion. This is due to the ‘holding’ feature of the bi-stable structure layers and the shape memory recovery property of the SMP matrix. The deployment process took 45 s. The dynamic deployment effect can be observed in supplementary video S3.

(3) Deploying test of the Bi-SMPC boom with heating layer: Figure 7(c) and supplementary video S4 show the deploying process of the boom with heating layer. The boom was

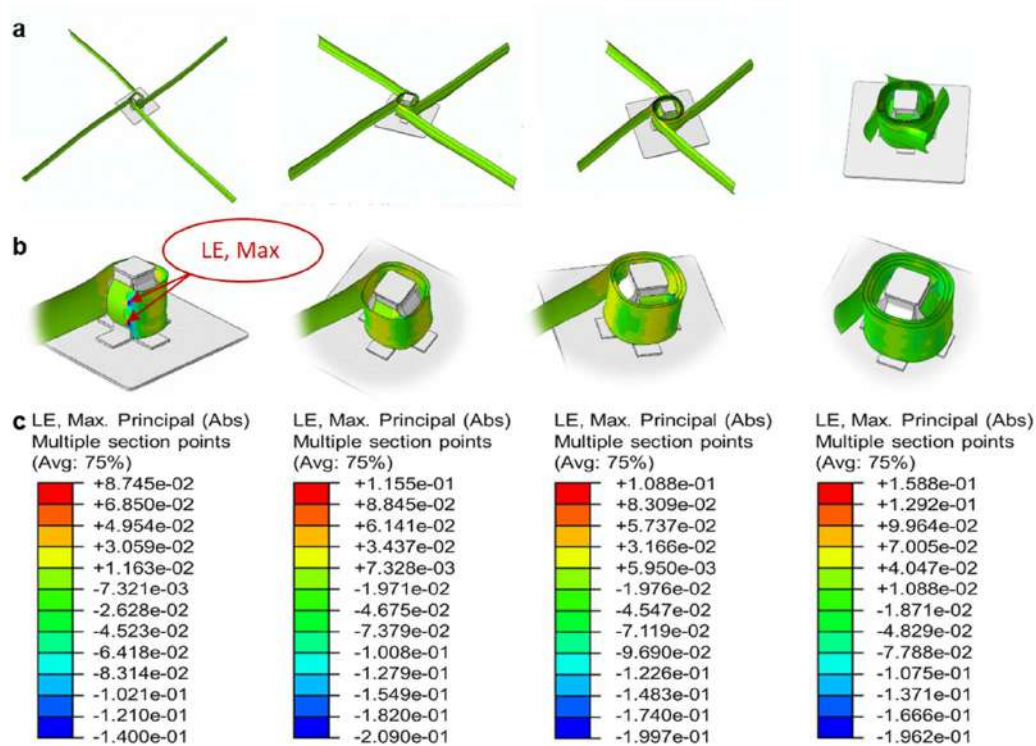


Figure 6. Logarithmic strain in the process of folding. (a) Four-step folding process of the simplified drag sail in the simulation; (b) and (c) strain of a single Bi-SMPC boom during the folding process.

fixed in a cantilever condition. A voltage of 20 V was used to drive the deployment of the four-stage Bi-SMPC boom controlled by an Arduino-based control board. The heating time for each stage was set to 90 s and the total time of the four-stage deployment procedure was 360 s. At the time of 410 s, the boom was cooled down to room temperature and returned to straight shape. However, it had a slight deflection of 14 mm compared to its original unfolded shape, which was reflected in an angular tilt of 1.88° at the tip.

To further test the stiffness of the boom, a 40 g weight (equivalent to 2.6 times the weight of the boom) was added to the tip for the deployment test, as shown in supplementary video S5. It was found that the boom still has good deployment capability when the tip is loaded, although the load generated a large deflection of 73 mm with an angle of 9.68° at the tip. When driven by heating layers, the deployment process is less steady than that in the oven because the heating layer does not heat the boom as uniformly as in the oven. Nevertheless, it is effective and controllable enough for use in deployable structures.

5.2. Deploying test of the drag sail

The folding and deploying process of the drag sail based on Bi-SMPC booms is shown in figure 8. The folding process

consists of four steps. Firstly, fold the four PI films and let them lean against the adjacent booms.

Secondly heat the four booms to the temperature around T_g and then rotate the booms clockwise around the central base to fold the drag sail. Thirdly cool down the booms to room temperature to maintain the folded shape. Fourthly connect each folded film to the tip of the adjacent boom with a spring connector, and then install the locking-release device. The deploying process starts with the execution of the heat driving control program to unlock the folded sail, followed by heating the booms to deploy the sail in four stages.

The drag sail was suspended by using a nylon rope during the deployment test. According to the drive parameters determined in the supplementary material (section S3), the heating procedure of the control board is set to turn on the heat-cut alloy wire of the locking-release device for 15 s to cut the locking rope and then sequentially heat each part of the Bi-SMPC booms for 180 s to deploy in four stages. Figure 9 shows the deployment process and the heating procedure of the drag sail, and the deployment video at ten times the speed can be seen in supplementary video S6. It can be found that the drag sail was successfully deployed in four stages in a slow and orderly manner, although the four booms appeared to deploy asynchronously due to the dispersion of the manufacturing process and the temperature field. It took about 12 min to deploy in total.



Figure 7. Deploying tests of the Bi-SMPC booms. (a) Folded state without heating circuit, folded state with the heating circuit, and deployed state of the Bi-SMPC booms, respectively; (b) deploying test of the Bi-SMPC boom in an oven; (c) deploying test of the Bi-SMPC boom driven by the heating layer at a voltage of 20 V.

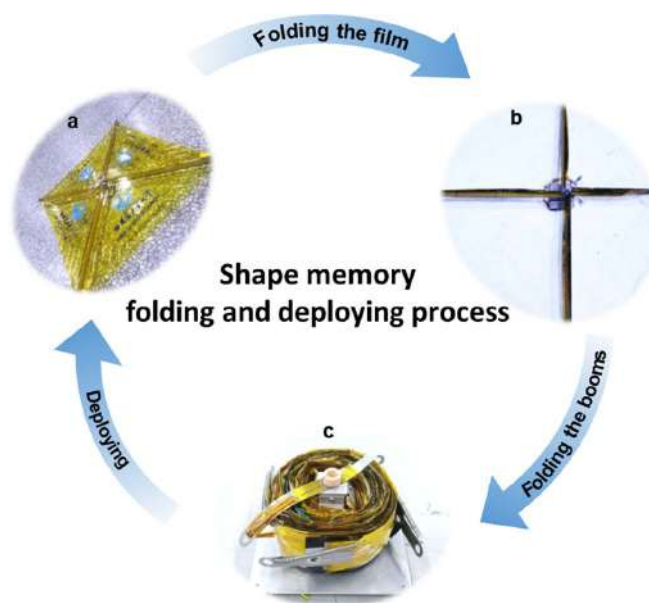


Figure 8. Shape memory folding and deploying process of the drag sail. (a) Deployed state of the drag sail; (b) half-folded state where each sail film has been folded, but the booms are not folded; (c) folded state of the drag sail.

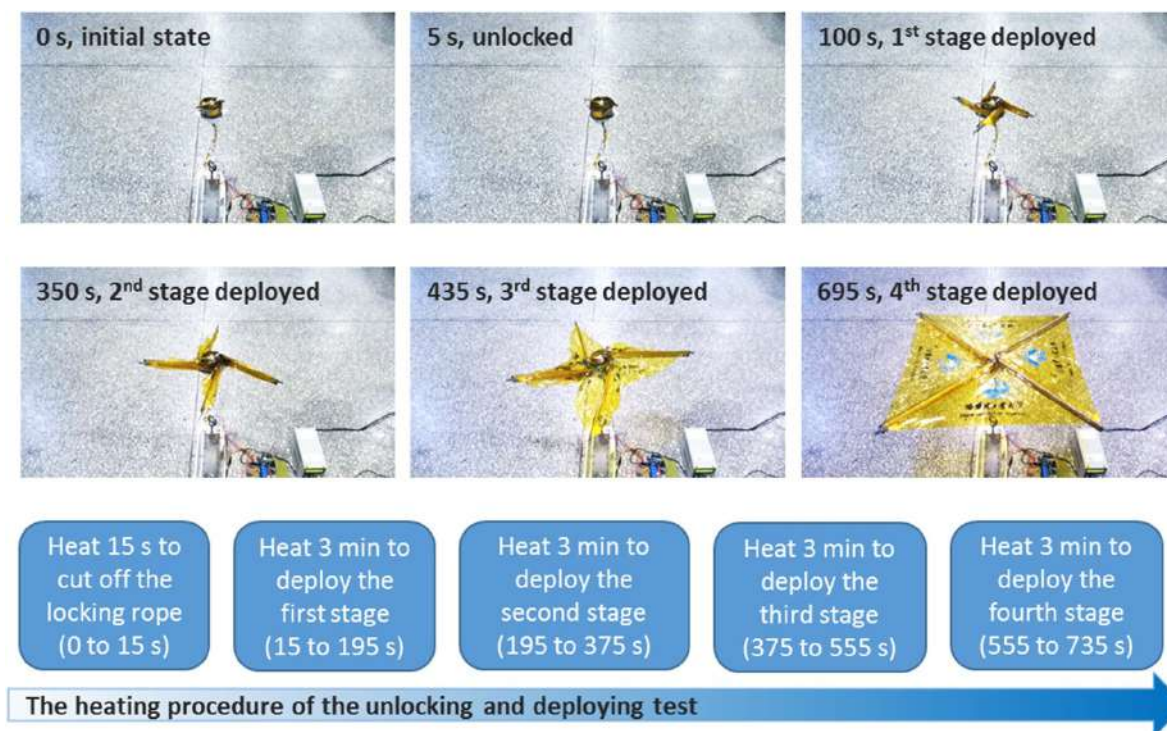


Figure 9. Deployment process of the drag sail.

6. Conclusions

An orderly roll-out, high storage ratio, and low-impact deployable Bi-SMPC boom was developed by using thermally driven SMP as the matrix to control the release of elastic energy stored in a bi-stable composite structure. Two resistive materials, carbon fiber yarn and Cr₂₀Ni₈₀ alloy wire, were tested and compared experimentally as the heating layers of the Bi-SMPC booms. The relationship between the two parameters, driving voltage and driving time, and the temperature field was investigated. Accordingly, the optimal driving strategy, voltage, and time were obtained. Ground tests were conducted to verify the stability and controllability of the Bi-SMPC booms, and a four-boom deployable drag sail was successfully deployed based on the deployable Bi-SMPC booms.

The main findings of this study are as follows: (1) SMPs can be used to achieve low-impact, controllable, and segmented deployment of bistable structures. This allows for more efficient and reliable deployment mechanisms. (2) The design strategy of a flexible nickel–chromium alloy resistance-driven layer has a uniform temperature field and can deform with the deformation of the boom. It can reliably drive the deployment of Bi-SMPC booms. (3) The drag sail designed in this study can be successfully deployed with the cooperation of four Bi-SMPC booms. This study provides a new idea for the development of space deployable structures. Meanwhile, the design and verification of the drag sail prototype will provide some technical reference for deorbiting, thus reducing space debris from the source.

Data availability statement

All data that support the findings of this study are included within the article (and any supplementary files).

Acknowledgments

This work was supported by the National Natural Science Foundation of China (Grant Number 12102107); the China National Postdoctoral Program for Innovative Talents (Grant Number BX2021090); and the International Space Science and Scientific Payload Competition Organizing Committee.

Conflict of interest

The authors declare that they have no known competing financial interests or personal relationships that could have appeared to influence the work reported in this paper.

CRedit author statement

Guangqing Ming: Conceptualization, Methodology, Investigation, Visualization, Writing- Original draft, Reviewing & Editing. **Siling Chen:** Methodology, Investigation. **Bingxun Li:** Investigation. **Fengfeng Li:** Methodology, Writing- Reviewing & Editing, Supervision. **Liwu Liu:** Project administration, Resources, Supervision. **Yanju Liu:** Resources, Funding acquisition. **Jinsong Leng:**

Supervision, Project administration, Resources, Funding acquisition, Writing- Reviewing & Editing.

ORCID iDs

Guangqing Ming  <https://orcid.org/0000-0002-7338-9155>

Liwu Liu  <https://orcid.org/0000-0002-7737-9827>

Yanju Liu  <https://orcid.org/0000-0001-8269-1594>

Jinsong Leng  <https://orcid.org/0000-0001-5098-9871>

References

- [1] ESA's Space Debris Office 2022 Space debris by the numbers (European Space Agency) (available at: www.esa.int/Space_Safety/Space_Debris/Space_debris_by_the_numbers) (Accessed 11 August 2022)
- [2] Anz-Meador P 2020 Orbital debris quarterly news (NASA Orbital Debris Program Office) 24
- [3] Kessler D J, Johnson N L, Liou J C and Matney M 2010 The kessler syndrome: implications to future space operations *33rd Annual AAS Rocky Mountain Guidance and Control Conf. (Breckenridge, CO, 05–10 February 2010)* vol 137 p 47
- [4] Li Y, Wang W, Li Z and Chen Y 2014 *Space Debris Removal* (National Defense Industry Press)
- [5] Liou J C 2010 The top 10 questions for active debris removal *Mol. Vision* **16** 756–67
- [6] Schaub H and Moorer D F 2012 Geosynchronous large debris reorbiter: challenges and prospects *J. Astronaut. Sci.* **59** 165–80
- [7] Johnson N L and Stansbery E G 2010 The new NASA orbital debris mitigation procedural requirements and standards *Acta Astronaut.* **66** 362–7
- [8] Macdonald M 2014 *Advances in Solar Sailing* (Springer)
- [9] Harkness P, McRobb M, Lutzendorf P, Milligan R, Feeney A and Clark C 2014 Development status of AEOLDOS—a deorbit module for small satellites *Adv. Space Res.* **54** 82–91
- [10] Hiemstra J M 2014 *Mechanical Design and Development of a Modular Drag Sail for the CanX-7 Nanosatellite Mission* (University of Toronto)
- [11] Fernandez J M, Visagie L, Schenk M, Stohlman O R, Aglietti G S, Lappas V J and Erb S 2014 Design and development of a gossamer sail system for deorbiting in low earth orbit *Acta Astronaut.* **103** 204–25
- [12] Wei J Z, Ma R Q, Liu Y F, Yu J X, Eriksson A and Tan H F 2018 Modal analysis and identification of deployable membrane structures *Acta Astronaut.* **152** 811–22
- [13] Lappas V, Adeli N, Visagie L, Fernandez J, Theodorou T, Steyn W and Perren M 2011 CubeSail: a low cost CubeSat based solar sail demonstration mission *Adv. Space Res.* **48** 1890–901
- [14] Fernandez J M, Lappas V J and Daton-Lovett A J 2011 Completely stripped solar sail concept using bi-stable reeled composite booms *Acta Astronaut.* **69** 78–85
- [15] Silver M, Hinkle J and Peterson L 2004 Modeling of snap-back bending response of doubly slit cylindrical shells *Proc. 45th AIAA/ASME/ASCE/AHS/ASC Structures, Structural Dynamics & Materials Conf.*
- [16] Walker S J I and Aglietti G S 2006 Experimental investigation of tape springs folded in three dimensions *AIAA J.* **44** 151–9
- [17] Yang H, Guo H W, Wang Y, Feng J and Tian D K 2020 Analytical solution of the peak bending moment of an M boom for membrane deployable structures *Int. J. Solids Struct.* **206** 236–46
- [18] Meng Q H and Hu J L 2009 A review of shape memory polymer composites and blends *Composites A* **40** 1661–72
- [19] Melly S K, Liu L, Liu Y and Leng J 2021 A review on material models for isotropic hyperelasticity *Int. J. Mech. Syst. Dyn.* **1** 71–88
- [20] Liu S and Yang Q-S 2019 Finite element analysis of shape-memory polymer mast *Int. J. Smart Nano Mater.* **10** 285–99
- [21] Zhao W, Zhu J, Liu L, Leng J and Liu Y 2023 A bio-inspired 3D metamaterials with chirality and anti-chirality topology fabricated by 4D printing *Int. J. Smart Nano Mater.* **14** 1–20
- [22] Ming G Q, Liu L W, Liu Y J and Leng J S 2023 Space deployable parabolic reflector based on shape memory polymer composites *Compos. Struct.* **304** 116327
- [23] Chen L, Li W B, Liu Y J and Leng J S 2016 Nanocomposites of epoxy-based shape memory polymer and thermally reduced graphite oxide: mechanical, thermal and shape memory characterizations *Composites B* **91** 75–82
- [24] Zhang F, Wen N, Wang L, Bai Y and Leng J 2021 Design of 4D printed shape-changing tracheal stent and remote controlling actuation *Int. J. Smart Nano Mater.* **12** 375–89
- [25] Guinot F, Bourgeois S, Cochelin B, Hochard C and Blanchard L 2009 Hybrid tape-springs for deployable hexapod *50th AIAA/ASME/ASCE/AHS/ASC Structures Structural Dynamics, and Materials Conf.*
- [26] Wang C G and Wang Y F 2018 The mechanical design of a hybrid intelligent hinge with shape memory polymer and spring sheet *Composites B* **134** 1–8
- [27] Shahryarifard M, Golzar M and Tibert G 2021 Toward thermal stimulation of shape memory polymer composite bistable tape springs *Smart Mater. Struct.* **30** 025030
- [28] Kwok K 2018 Viscoelastic analysis of stowage and quasi-static deployment of composite tape springs *Proc. 2018 AIAA Spacecraft Structures Conf.*
- [29] Luo L, Zhang F H and Leng J S 2021 Multi-performance shape memory epoxy resins and their composites with narrow transition temperature range *Compos. Sci. Technol.* **213** 108899
- [30] Li F, Leng J, Liu Y, Remillat C and Scarpa F 2020 Temperature dependence of elastic constants in unidirectional carbon fiber reinforced shape memory polymer composites *Mech. Mater.* **148** 103518
- [31] Zhang D, Liu L, Lan X, Li F, Liu Y and Leng J 2023 Experimental study on nonlinearity of unidirectional carbon fibre-reinforced shape memory polymer composites *Composites A* **166** 107372